Physical experiments of tsunami scour around on-shore square structures

Rafael Aránguiz[1,2], Javiera Dinamarca[1], Valentina Bravo[3], Oscar Link[3]

[1]Department of Civil Engineering, Universidad Católica de la Ssma Concepción, Alonso de Ribera 2850, Concepción, Chile; e-mail: raranguiz@ucsc.cl Corresponding author.
[2]Research Center for Integrated Disaster Risk Management (CIGIDEN)
[3] Department of Civil Engineering, Universidad de Concepción, Chile.

ABSTRACT

Estimation of the maximum scour depth is important for defining the size and depth of building foundations in order to avoid failure during a tsunami. Traditionally, tsunami scour has been studied in laboratory experiments that use solitary waves. However, new research carried out laboratory experiments of scour around a bridge pier by means of a pump-driven flow system, and the discharge as well as the flow depth were controlled. The present work analysed tsunami scour around an on-shore square structure in two different ways: first, in a 20m long wave flume with solitary waves, and second, in a 6m long wave flume and using a pump-driven flow method in order to represent more realistic tsunami waves. The tsunami hydrodynamic parameters were obtained from real scale numerical tsunami simulations. Preliminary results show that experiments at different scales are comparable and maximum scour depth is smaller than scour compute by means of current equations. In addition, there is a good agreement between the tsunami hydrodynamic features given by the pump driven flow system and the simulated tsunami parameters. However, the scour depth obtained from a pump driven flow method demonstrated that inundation time plays an important role on maximum tsunami scour, which is much larger than previous results and exceed scour predicted by current equations.

INTRODUCTION

Tsunamis can generate significant damage to coastal structures such as seawalls, coastal dikes, bridges and buildings. The causes of structural failure of these types of structures, which are subjected to tsunami loads, can be categorized into four groups: 1) hydrostatic and hydrodynamic forces, 2) impact forces by debris, 3) fire spread by floating materials (including burning oil), and 4) scour and foundation failure. Scour is defined as "removal of soil or fill material by the flow of floodwaters, frequently used to describe storm-induced, localized conical erosion around pilings and other foundation supports where the obstruction of flow increases turbulence" (FEMA, 2012). Tsunamis can mobilize large amounts of soil substrate, generating scouring of structural

foundations, slope instability failures and liquefaction failures (Tonkin et al., 2003). Subsequently, scouring may expose building foundations and cause global failure of the structure.

The ability to predict the scour depth around structures under tsunami attack, such as protective structures and tsunami evacuation buildings, is very important in designing the foundations and avoiding failure. After the 2004 and 2011 tsunami events, the scour around coastal dykes and seawalls have been extensively studied. These studies proposed the tsunami scour depth as a function of the flow depth (Jayaratne et al., 2016; Tonkin et al., 2003). Tsunami scour around buildings is found less in literature and design methods suggest that scour may be computed as a percentage of the flow depth, depending on the soil type and distance from the shore (FEMA, 2012). Yeh et al., (2012) argued that tsunami scour is not only caused by shear and hydrodynamic uplift forces, which require high velocity flows to generate scour. Rather, it is likely that uplift force caused by pore pressure gradient due to the rapid reduction of the flow depth, i.e. pore pressure gradient, triggers momentary liquefaction in some locations and subsequently, soil instability (Yeh & Manson, 2014). Therefore, soil instabilities, and subsequently severe scour are not always the result of fast and violent flows.

Early research on tsunami scour was based on experiments in laboratory prototypes with slender cylinder using solitary waves (Moronkeji et al., 2007; Tonkin et al., 2003; Yeh et al., 2001). One of the most important findings is that pore pressure is the key factor of tsunami scour, thus during the drawdown process, the vertical pressure gradient around the cylinder decreases the effective stress within the soil and momentary liquefaction occur. However, this effect depends on the substrate. While gravel is more affected by greatest flow velocities and subsequently shear stress, sand experiences rapid scour during drawdown as a result of pore pressure gradient (Tonkin et al., 2003). In a similar manner, Nakamura et al., (2008) applied the same kind of experiments to study scour around a land-based square structure on a sandy beach. They found that scour holes around the seaward corner of the structure should be analysed considering both flow velocity and effective stress. The solitary wave laboratory experiments of Tonkin et al., (2003) have been used to validate numerical models. For example, Yeh & Manson, (2014) used a hybrid analytical-numerical approach to analyse a tsunami on a beach and compute velocities and depths, and proposed a modified shield parameter to account for the effect of pore pressure gradients. The results corroborated that pore pressure effect was substantial and became important for soil instability in the coastal environment. In a similar manner, Pan & Huang, (2012) developed a numerical model to study tsunami scour around a circular cylinder. In general, the numerical model coincided with experimental results of Tonkin et al., (2003). Recently, the excess pore water pressure gradient due to tsunami loading has been studied by means of numerical experiments in a coupled seepage-deformation model (Abdollahi & Mason, 2019b, 2019a, 2020a, 2020b). They run numerical

experiments with tsunami duration up to 60 min and found that the shorter the period the larger the pore water pressure gradient.

Objective of the present research is to compare results of tsunami scour with solitary wave and a new method using a pump-driven flow method. This work is organized as follows, The second section presents the methodology, then the results and discussions are presented, and the last section contains the main conclusion of this research.

METHODOLOGY

Two sets of experiments were performed. The first experiment considered a solitary wave in a 20 m wave flume in order to analyze and compare results with previous research. The wave flume has a width of 0.77m. The current experiment reproduced the experiment of April-LeQuéré et al., (2022), but using a 1:100 scale. Therefore, the water depth was 30cm. Some modifications were introduced in order to represent a typical Chilean city, such as Viña del Mar. A sloping beach of 5% (1:20) in the sea side and 10% (1:10) in the land side followed by a horizontal surface at 3,5cm ground elevation were used, as shown in Figure 1-a and b. The experiment set up is similar to the one used by McGovern et al., (2019). A transparent square column of 7cm was installed at a distance of 5cm from the shoreline. Three cameras were installed to record flow depth behaviour and scour, one at the top to record the flow around the column, one at one side of the flume to record the flow depth and one inside the column to record the scour. The solitary wave was generated by means of a piston-type wave generator. The maximum stroke of the equipped paddle is 0.85m. Four different solitary waves were tested, namely H=5.4, 7.5, 8.5 and 11.5m. In addition, each wave was repeated 4 times. The wave amplitude was measured by an ultrasonic sensor located at the beginning of the sloping beach. A graded sand with d_{50}=0.56mm was used to measure the scour depth.

The second experiment was carried out in a flume that is 6m long by 0.4m wide (See Figure 1-c). This flume has already been used to run experiments on scour around bridge piers (Link et al., 2018). The flume is implemented with a 0.6m long sediment recess located 4 m downstream of the flume entrance with a solid square cylinder of 2.9cm installed in the middle. The scour was monitored with a snake video camera that is 7mm in diameter, with a resolution of 640 by 480 pixels. The images were captured at a 0.2Hz frequency. The pump capacity is 25 l/s with a variable frequency driven by a logic programmable controller, thus any desired hydrograph shape is generated. The flow depth is controlled by an automatized tailgate at the end of the flume and measured with a precision of ±0.1 mm using an ultrasonic distance sensor. The tsunami wave is scaled from a tsunami numerical simulation of Coquimbo City, in northern Chile (Klapp et al., 2020). The maximum flow depth in the real scale simulation was 5.9m with an inundation stage of 300s. The laboratory scale was 1:70, therefore, the maximum flow depth was 8.5cm and the

inundation stage was 35s. Since the flume was designed to carry out experiments on bridge piers, it is not possible to reproduce the return flow of the tsunami, therefore, the experiments analyzed only the inundation stage of the phenomenon and subsequently, the variables which govern the scour process during this stage.

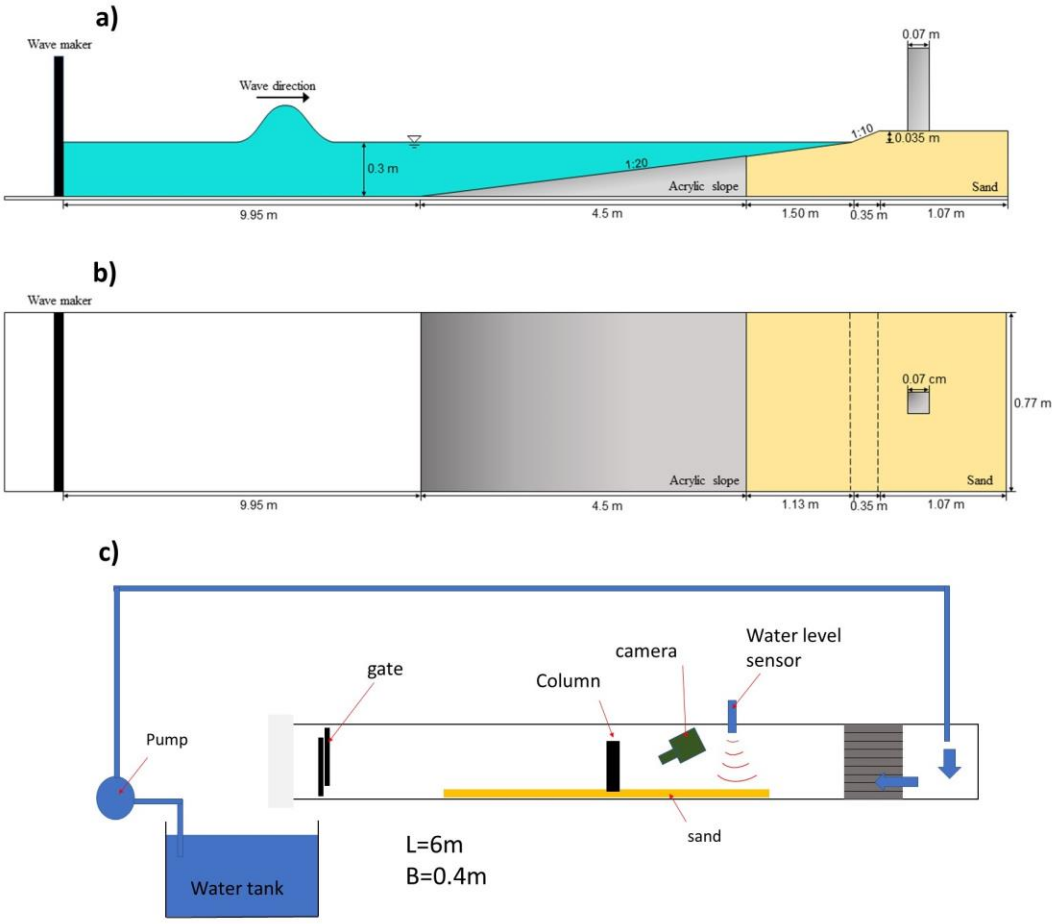

Figure 1. Setup of laboratory experiments. a) Elevation view of 20m wave flume and solitary wave. b) plan view of 20m wave flume. c) Elevation view of 6m wave flume and pump-driven flow method.

RESULTS AND DISCUSSION

Figure 2 shows snapshot of inundation and scour depth for solitary wave experiments. From the Figure, it is possible to observe that the inundation lasts only 5s, and the scour increased rapidly as a function of time. It is observed that the scour at the corner of the structure is deeper than the scour at the center. This result is consistent with results given by McGovern et al., (2019) and Nakamura et al., (2008). In addition, despite the setup did not allow large amount of return flow, the final scour at the corner (t=19s) showed to be smaller than the maximum scour (t=11s). By

means of theses videos, it was possible to measure the maximum scour at both the center and the corner of the square cylinder.

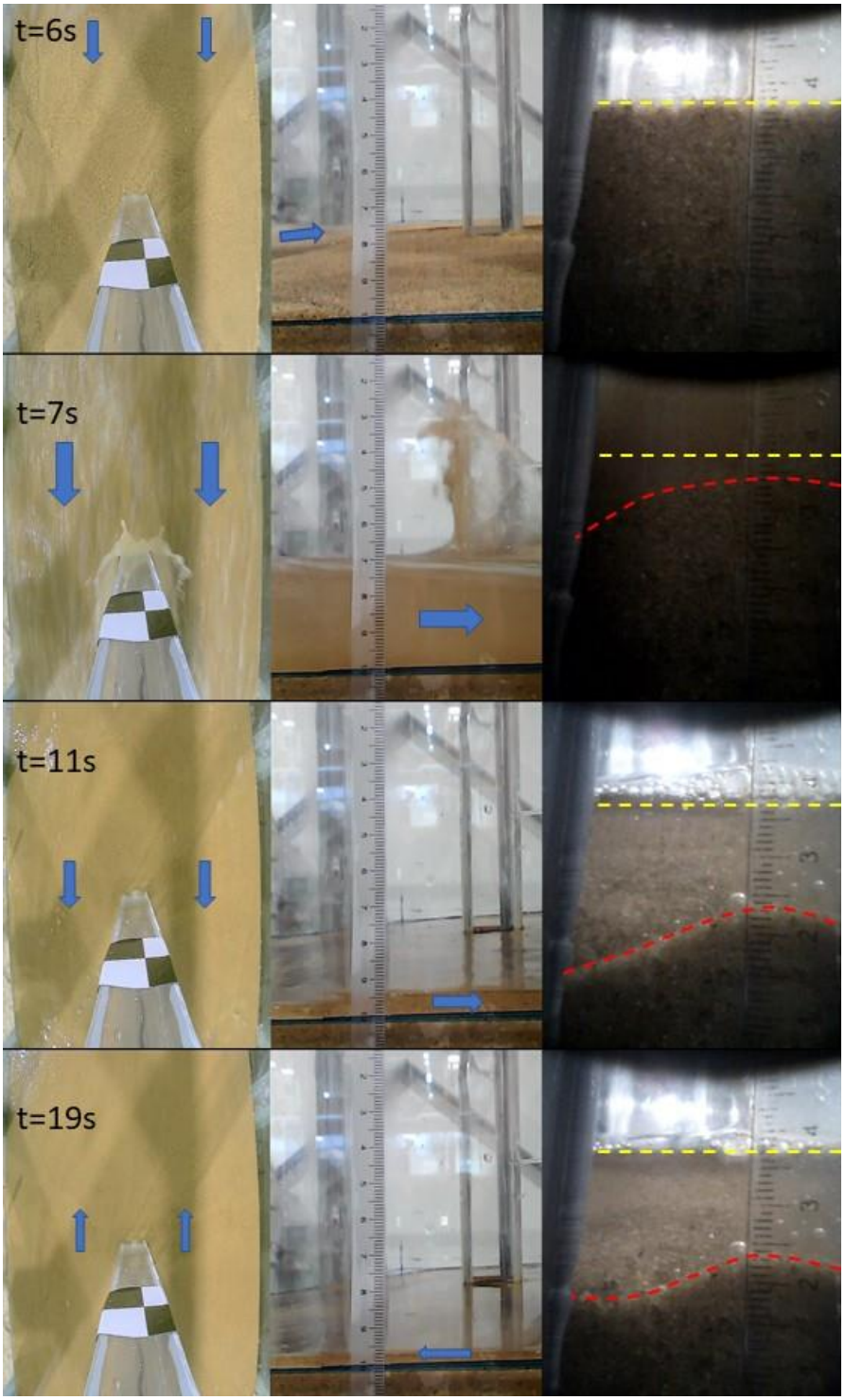

Figure 2. Snapshot of inundation and scour for a solitary wave in the 20m wave flume. Yellow line represents the original sand bed while the red line represents the instantaneous sand bed

Figure 3 shows examples of maximum scour for the two setups. The first row corresponds to experiments in the 20m wave flume with solitary waves. It is possible to observe that the scour around the structure has similar pattern to the one given by previous research, i.e. larger scour in the front side and accumulation in the back side. In addition, maximum scour is observed to be at the corner of the structure. A different result is observed in the 6m wave flume with the pump-driven flow method. Larger scour area is observed around the structure, which is more similar to scour around bridge piers, where no accumulation area is observed right back the cylinder, and more uniform scour depth is observed in the front side. In addition, the scour in the pump-driven flow method showed to be larger than the scour with solitary wave. Therefore, the inundation time seems to play an important role in the maximum tsunami scour depth.

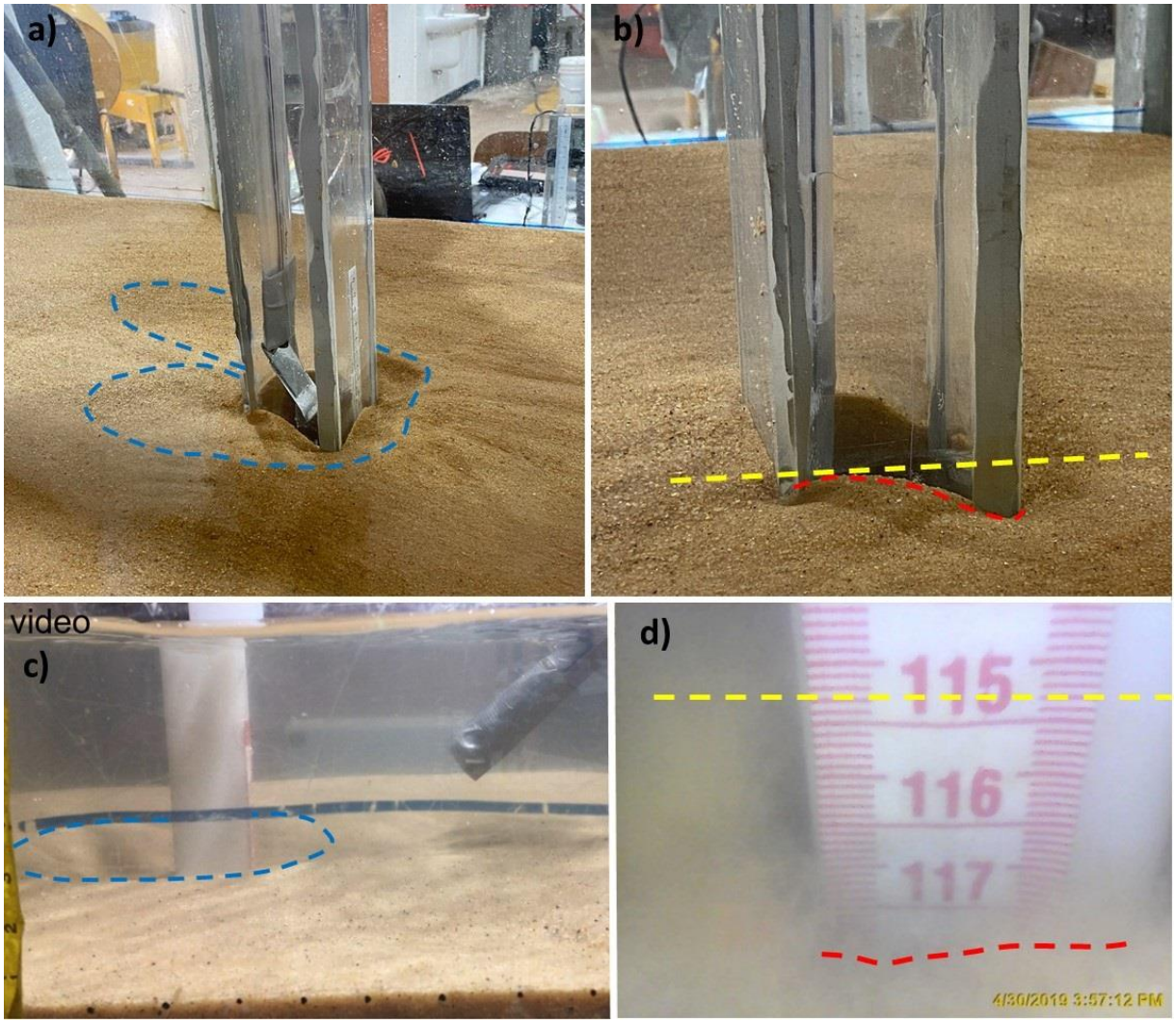

Figure 3. Example of results of tsunami scour. a) and b) are results for solitary wave in the 20m wave flume. c) and d) are results for pump-driven flow method in the 6m wave flume. In both cases, blue dashed lines represent the limit of the scour area around the structure, yellow line is the original level of sand bed, and red line is the maximum scour depth.

Figure 4 shows results of all the experiments carried out in the 20m wave flume. Figure 4-a shows the relationship between the wave amplitude and the flow depth. It is possible to observe that there is a linear relationship, such that the larger the wave amplitude, the larger the flow depth. However, for the largest waves, the flow depth becomes up to four times smaller than the original wave amplitude. Similar relationship is observed between the wave amplitude and the maximum scour depth (Figure 4-b). It is also possible to observed that the difference between scour at the corner and the center increased as the wave amplitude increased, i.e. smaller waves generate more uniform scour around the square cylinder. Figure 4-c shows a comparison of the solitary wave results with the equation given by the ASCE 7-16 Standards (blue line) in terms of the flow depth and the normalized maximum scour, in which B is the width of the square cylinder. The red square represents the result with the long wave in the 6m wave flume. To do this analysis, both the equation and the 6m wave flume result were scaled to the size of the 20 m wave flume experiments. It is possible to observe that all results with solitary waves are below the ASCE 7-16 equation, however, the long wave generated a much deeper scour depth. Subsequently, it would be necessary to analyze other variables such as the inundation time and velocity.

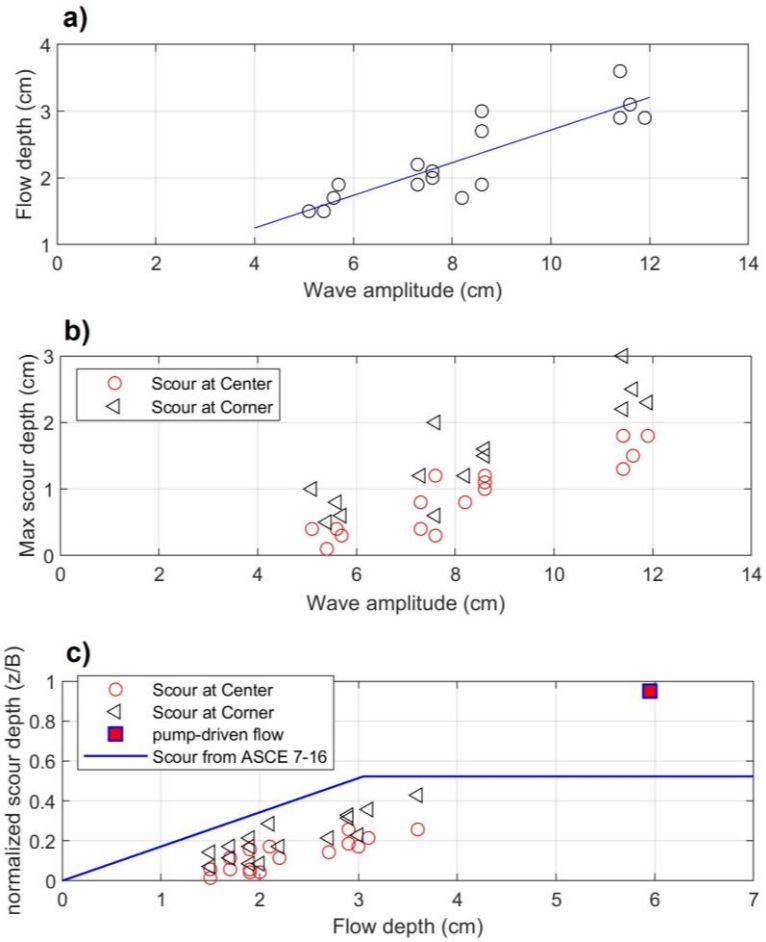

Figure 4. Results of tsunami scour experiment in the 20m wave flume. a) Wave amplitude v/s Flow depth. b) Wave amplitude v/s Maximum scour depth. c) Normalized scour depth as a function of Flow depth

Finally, Figure 5 shows a comparison of the current experiments with previous research reported in the work of McGovern et al., (2019). All results are normalized by the width of the square cylinder. In general, it is possible to observe that most of the results are comparable and they are below the ASCE 7-16 equation, including both solitary waves of the current research and long waves from Nakamura et al., (2008) and McGovern et al., (2019). The exception is the scour from the long wave in the pump-driven flow method of the current research, which is much larger than previous results. Despite the work of Nakamura et al., (2008) also used large amplitude waves, the maximum scour is relatively small. It may be due to the steeper slope (1/10) and the sea wall used in the experiments, which may cause reflection and/or energy loss, thus the flow had less scour potential.

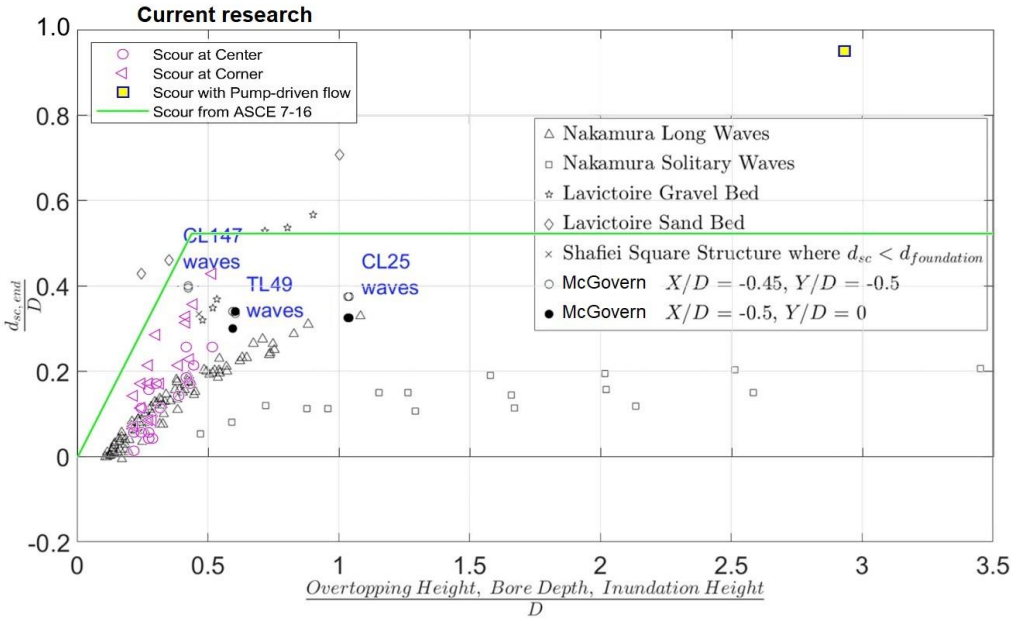

Figure 5. Comparison of current research and selected published experiments as a function of h/D and d/D, where D is the width of the squared cylinder, and d is the scour depth. Modified from McGovern et al., (2019)

The scour observed in the current research showed similar results of previous published research. For instance, the vertical vortices forming at the corners of the square cylinder have also been observed by McGovern et al., (2019) and were related to the large sediment transport near the corners. In addition, for short solitary waves, the scour pattern showed an accumulation of sediment at the back side of the squared cylinder, similar to the findings of Nakamura et al., 2008). It was observed that the inundation time has an important role on scour rather than the inundation height (flow depth). These results are consistent with observations from McGovern et al., (2019) by comparing their solitary wave data to their long wave data. This observation is more evident when the long wave from the pump-driven flow method is analyzed, due to the fact that long

inundation time and large wave amplitude can cause larger scour depth. Finally, all compared experiments used sand of different grain size (d_{50}), therefore, it is necessary to analyze the influence of this parameter in future research.

CONCLUSION

The present research analysed experiments of tsunami using solitary waves and long waves by means of a pump-driven flow method. Preliminary results show that experiments at different scales are comparable and maximum scour depth is smaller than scour compute by means of current equations when solitary waves. In addition, there is a good agreement between the tsunami hydrodynamic features given by the pump-driven flow system and the simulated tsunami parameters. In general, it was observed that current and previous results are comparable and they are below the ASCE 7-16 equation, including experiments with both solitary waves and long waves. The exception is the scour from the long wave in the pump-driven flow method of the current research, which is much larger than previous results. This result demonstrated that inundation time plays an important role on maximum tsunami scour, which is much larger than previous results and exceed scour predicted by current equations. Future research may focus the study on the experiments with long waves which are more representative of real tsunami waves. In addition, the effect of grain side should be analysed in order to investigate the real effect of pore pressure on tsunami scour.

ACKNOWLEDGEMENTS

The author would like to thank the ANID/FONDECYT 1210496 grant as well as the ANID/FONDAP 1522A0005-2022 grant for the Research Center for Integrated Disaster Risk Management (CIGIDEN).

REFERENCES

Abdollahi, A., & Mason, H. B. (2019a). Coupled Seepage-Deformation Model for Predicting Pore-Water Pressure Response during Tsunami Loading. *Journal of Geotechnical and Geoenvironmental Engineering*, *145*(3–04019002). https://doi.org/10.1061/(ASCE)GT.1943-5606.0002012

Abdollahi, A., & Mason, H. B. (2019b). Tsunami-induced pore water pressure response of unsaturated soil beds : Numerical formulation and experiments. *Computers and Geotechnics*, *110*, 19–27. https://doi.org/10.1016/j.compgeo.2019.02.012

Abdollahi, A., & Mason, H. B. (2020a). Estimating tsunami-induced uplift pressure. *Géotechnique Letters*, *10*, 1–21. https://doi.org/10.1680/jgele.19.00104

Abdollahi, A., & Mason, H. B. (2020b). Pore Water Pressure Response during Tsunami Loading. *Journal of Geotechnical and Geoenvironmental Engineering*, *146*(3–04020004).

https://doi.org/10.1061/(ASCE)GT.1943-5606.0002205
April-LeQuéré, P., Nistor, I., Mohammadian, A., Schimmels, S., Schendel, A., Goseberg, N., Welzel, M., Krautwald, C., & Stolle, J. (2022). Hydrodynamics and Associated Scour around a Free-Standing Structure Due to Turbulent Bores. *Journal of Waterway, Port, Coastal, and Ocean Engineering*, *148*(5), 1–17. https://doi.org/10.1061/(asce)ww.1943-5460.0000717
FEMA. (2012). *FEMA P-646: Guidelines for Design of Structures for Vertical Evacuation from Tsunamis*. https://www.fema.gov/media-library/assets/documents/14708
Jayaratne, M. P. R., Premaratne, B., Adewale, A., Mikami, T., Matsuba, S., Shibayama, T., Esteban, M., & Nistor, I. (2016). Failure Mechanisms and Local Scour at Coastal Structures Induced by Tsunami. *Coastal Engineering Journal*, *58*(4), 1640017-1-1640017–1640038. https://doi.org/10.1142/s0578563416400179
Klapp, J., Areu-Rangel, O. S., Cruchaga, M., Aránguiz, R., Bonasia, R., Godoy, M. J., & Silva-Casarín, R. (2020). Tsunami hydrodynamic force on a building using a SPH real-scale numerical simulation. *Natural Hazards*, *100*(1). https://doi.org/10.1007/s11069-019-03800-3
Link, O., Henríquez, S., & Ettmer, B. (2018). Physical scale modelling of scour around bridge piers. *Journal of Hydraulic Research*, *57*(2), 227–237. https://doi.org/10.1080/00221686.2018.1475428
McGovern, D. J., Todd, D., Rossetto, T., Whitehouse, R. J. S., Monaghan, J., & Gomes, E. (2019). Experimental observations of tsunami induced scour at onshore structures. *Coastal Engineering*, *152*(January), 103505. https://doi.org/10.1016/j.coastaleng.2019.103505
Moronkeji, A., Hinsdale, O. H., & Young, Y. L. (2007). Physical modelling of tsunami induced sediment transport and scour. *Proceedings of the 2007 Earthquake Engineering Symposium for Young Researchers*, 1–15.
Nakamura, T., Kuramitsu, Y., & Mizutani, N. (2008). Tsunami Scour Around a Square Structure. *Coastal Engineering Journal*, *50*(2), 209–246. https://doi.org/10.1142/s057856340800179x
Pan, C., & Huang, W. (2012). Numerical Modeling of Tsunami Wave Run-Up and Effects on Sediment Scour around a Cylindrical Pier. *Journal of Engineering Mechanics*, *138*(10), 1224–1235. https://doi.org/10.1061/(asce)em.1943-7889.0000406
Tonkin, S., Yeh, H., Kato, F., & Sato, S. (2003). Tsunami scour around a cylinder. *Journal of Fluid Mechanics*, *496*(496), 165–192. https://doi.org/10.1017/S0022112003006402
Yeh, H., Kato, F., & Sato, S. (2001). Tsunami Scour Mechanisms around A Cylinder. In G. T. Hebenstreit (Ed.), *Advances in Natural and Technological Hazards Research* (p. 282). Springer-Science+Business Media. https://doi.org/10.1007/978-94-017-3618-3
Yeh, H., & Manson, H. B. (2014). Sediment response to tsunami loading: mechanisms and estimates. *Géotechnique*, *64*(2), 131–143. https://doi.org/10.1680/geot.13.p.033
Yeh, H., Sato, S., & Tajima, Y. (2012). The 11 March 2011 East Japan Earthquake and Tsunami: Tsunami Effects on Coastal Infrastructure and Buildings. *Pure and Applied Geophysics*, *170*(6–8), 1019–1031. https://doi.org/10.1007/s00024-012-0489-1